Introduction to a performance-based design method for rocking shallow foundations in seismic zone

Keshab Sharma, PhD
BGC Engineering Inc., Fredericton, NB,
Jia Bin, PhD
College of Civil Engineering, Hunan University of Technology, Zhuzhou, Hunan, China
Lijun Deng, PhD, Peng.
Department of Civil and Environmental Engineering, University of Alberta, Edmonton, AB, Canada

ABSTRACT
This paper proposes a performance-based seismic design (PBSD) methodology for design of rocking shallow foundations for ordinary bridges in cohesive soils. This PBSD considers three performance indicators: maximum drift, residual footing rotation and residual settlement. The empirical equations of re-centering ratio and residual settlement obtained from field testing program of rocking foundation were adopted to check the performance in terms of residual drift and residual settlement. Empirical correlations to obtain the secant stiffness, hysteresis damping ratios, re-centering ratio and residual settlement were obtained from preceding field tests. The shallow foundation of as-built Sanguinetti Bridge, Sonora County, California, was re-designed for assumed cohesive soil sites in British Columbia. It is observed that the foundations of Sanguinetti Bridge can be designed reasonably well using the PBSD while satisfying the performance criteria for 2% maximum drift, residual drift, and residual settlement. The performance of the re-designed bridge was further validated using nonlinear time history analyses. The finite element model was developed in OpenSees platform, validated against the field test results.

RÉSUMÉ
Cet article propose une méthodologie de conception sismique basée sur la performance (PBSD) pour la conception de fondations basculantes peu profondes pour des ponts ordinaires dans des sols cohésifs. Ce PBSD considère trois indicateurs de performance: la dérive maximale, la rotation de la semelle résiduelle et le tassement résiduel. Les équations empiriques du rapport de recentrage et du tassement résiduel obtenues à partir du programme d'essais sur le terrain des fondations basculantes ont été adoptées pour vérifier les performances en termes de dérive résiduelle et de tassement résiduel. Des corrélations empiriques pour obtenir la rigidité sécante, les rapports d'amortissement d'hystérésis, le taux de recentrage et le tassement résiduel ont été obtenues à partir des essais sur le terrain précédents. Les fondations peu profondes du pont Sanguinetti tel que construit, dans le comté de Sonora, en Californie, ont été remodelées pour des sols supposés cohésifs en Colombie-Britannique. On observe que les fondations du pont Sanguinetti peuvent être raisonnablement bien conçues en utilisant le PBSD tout en satisfaisant aux critères de performance pour une dérive maximale de 2%, une dérive résiduelle et un tassement résiduel. Les performances du pont redessiné ont été validées à l'aide d'analyses chronologiques non linéaires. Le modèle par éléments finis a été développé sur la plate-forme OpenSees, validé par rapport aux résultats des tests sur le terrain.

1 INTRODUCTION

Shallow foundation is commonly used to support bridges and building structures. Shallow foundation supports about 40% bridges in BC and 17% of bridges in 39 states in the USA (NCHRP 2010; Siddiquee and Alam 2017). Shallow foundations are conventionally designed as a fixed base. Conventionally, the period of the structure is assumed relatively small, which leads to a large base shear and moment as the lengthening of period of system and increasing damping due to soil nonlinearity are not considered (AASHTO 2011; CSA 2014). A large footing size is required for large base shear and moment. An ultimate moment at the footing is calculated by multiplying the ultimate moment capacity of column by an overstrength factor greater than 1.3 (Gazetas 2019). Conventional footing design permits eccentricity due to seismic loading to fall within the middle two-third of the footing, which leads to excessively large footing.

Rocking shallow foundations with reduced capacity have demonstrated advantages over conventional fixed-base foundation under seismic loading. The fundamental of rocking foundation has been accepted in the building codes of several countries (CSA 2014; EGBC 2018; NZS 2004). In the USA, FEMA 440 (FEMA 2005) and ASCE 41-13 (ASCE 2014) incorporate rocking foundation effects by considering an increased period and a modified damping of the system. Rocking foundation may be permitted under seismic loading provided that foundation soils are not susceptible to loss of strength under the imposed cyclic loading (AASHTO 2011).

The performance-based seismic design (PBSD) defines the allowable displacement of earth structures and is commonly practiced in geotechnical earthquake engineering (Finn 2018). Various PBSD approaches based

on direct displacement-based design (DDBD) were developed to control the lateral displacements of structures (Sadan et al. 2013) under a specified design earthquake (Billah and Alam 2016). Although PBSD can be potentially useful for shallow foundations, limited research on PBSD for rocking foundation system have been conducted so far.

Algie (2011) and Deng et al. (2014) proposed a DDBD methodology for the seismic design of rocking shallow foundations for shear wall and ordinary bridges respectively. Both of them defined the performance level of the structure in terms of drift limits and involved the complicated process to calculate the initial stiffness, yield rotation, hysteresis, and radiation damping. Performance levels which are the backbone of the PBSD were not defined and checked in Algie (2011). More recently, the field behaviour of rocking foundations with large rotation (~7%) in cohesive soil was investigated (Sharma and Deng 2019, 2020 and 2011). The empirical relationships for the performance indicators developed in field tests can be potentially implemented in the PBSD of rocking foundations.

The aim of this research is to develop a PBSD framework for rocking shallow foundation in cohesive soils using three performance indicators: the allowable maximum and residual drift, and residual settlement. In this design procedure, a bridge system consisting of a rocking foundation, a damped elastic column, and a deck mass is integrated into a single-degree-of-freedom system for which the system damping, and period are calculated. One design example is presented with realistic values to show the feasibility of PBSD. Performance of the soil-footing-structure system was validated using a numerical model developed in the OpenSees platform. The proposed PBSD method is applicable to standard ordinary bridges and may be extended to multi-span bridges and multi-story buildings.

2 INPUT PARAMEERS

Input parameters of the PBSD are derived from empirical equations obtained from field experiment of rocking system. A single pier consisting of a rocking foundation was built and tested in a cohesive soil site in Edmonton, Canada (Sharma 2019). The system consisted of a 1.5 m by 1.0 m concrete footing, steel column and deck. Foundation rocking was induced in lateral snap-back or cyclic loading tests. The soil in the site can be classified as MH according to Unified Soil Classification System (USCS). Empirical correlations for secant stiffness, hysteresis damping ratios, re-centering ratio and residual settlement were hence developed, which will be used by the present PBSD method (Sharma 2019).

2.1 Damping Ratio

The total damping of the soil-foundation-structure system can be split into structural damping, ξ_p and foundation damping, ξ_f. The foundation damping is the contribution of hysteresis damping, ξ_{hys} (i.e., material damping) and radiation damping, ξ_r. Ambrosini (2006) and Adamidis et al. (2014) revealed that ξ_f would rarely exceed 2%. The yielding of soil reduces the energy dissipation through the outgoing waves. As a result, ξ_r of nonlinear soil is significantly less than that of elastic soil. As such, ξ_{hys} is taken as ξ_f. Then, the system damping (ξ_{sys}) can be calculated using Equation 1 (Sullivan et al. 2010; Algie 2011):

$$\xi_{sys} = \frac{\xi_{hys}\Delta_f + \xi_p\Delta_p}{\Delta_f + \Delta_p} \quad [1]$$

where Δ_f and Δ_p are the footing displacement due to rocking and sliding, and structural displacement of pier respectively.

CSA (2014) suggests that damping of the isolation system used in the design and analysis be based on field tests. The field tests of rocking shallow foundation in cohesive soil showed that the damping of the soil-foundation system was significantly greater than the 5% (Sharma and Deng 2020) as shown in Figure 1. The damping throughout the field tests ranged from 8 to 30%.

2.2 Secant Stiffness

In order to develop a rotational stiffness reduction trend, the normalized secant stiffness ($\overline{K}_{\text{sec}}$) was introduced in Chatzigogos et al. (2011), as defined in Equation 2:

$$\overline{K}_{\text{sec}} = \frac{K_{\text{sec}}}{Q \cdot L_{\text{f}}} = \frac{M_{\max}}{\theta_{\text{f}} \cdot Q \cdot L_{\text{f}}} \quad [2]$$

where $M_{\max}$ = maximum rocking moment; θ_f = maximum footing rotation; Q = vertical load on the foundation; and L_f = footing length along the rocking direction.

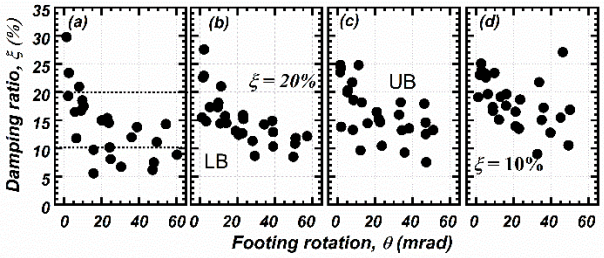

Figure 1. Hysteresis damping ratio versus amplitude of rotation for all tests with different A/A_c ranges: (a) 17-24, (b) 10-17, (c) 7-10, and (d) 5-7. UB = upper bound; LB = lower bound.

Figure 2 shows the distribution of $\overline{K}_{\text{sec}}$ vs. θ_f that was proposed by Sharma and Deng (2020). It is seen that the $\overline{K}_{\text{sec}}$ distribution becomes much more condensed and is almost unique at greater θ_f regardless of the A/A_c ratio or loading direction. The effect of the A/A_c ratio or loading direction on $\overline{K}_{\text{sec}}$ is not considered in this research. Sharma and Deng (2020) proposed the best estimate of $\overline{K}_{\text{sec}}$ vs. θ_f correlation for cyclic loading tests:

$$\overline{K}_{\text{sec}} = 1.4\theta_{\text{f}}^{-0.7} \quad [3]$$

The selection of $\overline{K}_{\text{sec}}$ empirical correlation affects the estimation of K_{sec} in Equation 2 and thus the subsequent

design. The effect of $\bar{K}_{sec}$ on the foundation design will be further elucidated.

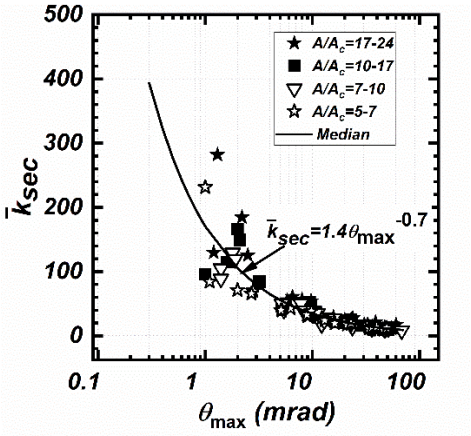

Figure 2. Normalized rocking stiffness vs. maximum footing rotation and (Sharma and Deng 2020).

3 PERFORMANCE INDICATORS

PBSD assesses the post-earthquake performance based on displacements instead of accelerations (or forces). This section describes the selection of performance indicators: maximum and residual drift, and rocking-induced residual settlement. The reason is that these parameters can be related to the damage level of the systems and helps decide whether a bridge can be re-opened after an earthquake (Billah and Alam 2016).

3.1 Maximum and Residual Rotation

The maximum lateral displacement (Δ_d) at the deck should be first selected in the PBSD to achieve a target performance level (Sadan et al. 2013). The value of Δ_d (Figure 2) could be the sum of structural displacement (Δ_p), footing sliding (Δ_{sl}) and rocking induced lateral displacement (Δ_r). Selection of Δ_d could be based on the drift, *P-Δ* moment limit, performance level of the seismic hazards, space needed to avoid building pounding, minimum seating width of abutment for bridge, and importance of the structures. NBCC (2010) limits the maximum drift ratio, γ_m to 2% for high importance building and 2.5% for general buildings. AASHTO (2011) tolerates γ_m of 4%. For conventional pier system, both CSA (2019) and Caltrans (2019) limit the P-Δ moment to 0.25M_{c_p}, where M_{c_p} is the design moment capacity of the pier.

ASCE (2014) and CSA (2019) define the performance level in term of residual drift after a seismic event; for example, a lifeline structure should be operational with limited service at the selected seismic hazard level to meet the performance requirement. To achieve the operational performance level, a target residual drift ratio (γ_{res}) of 0.6% is assumed for a lifeline bridge (Billah and Alam 2016; CSA 2019). In the present research, the re-centering ratio is used to estimate the residual rotation, which was introduced by Deng et al. (2014):

$$R_d = 1 - \frac{\theta_{res}}{\theta_f} \quad [4]$$

where θ_{res} is the residual foot rotation at zero rocking moment and θ is the design footing rotation (i.e., maximum footing rotation). The value of θ_{res} is equal to γ_{res} of the system since the pier remains elastic. The empirical equation of R_d vs. A/A_c curve (in Figure 4) developed by Sharma and Deng (2020) from the field test in cohesive soil is used in this research as follows:

$$R_d = \frac{1}{2.055\frac{A_c}{A}+1.015} \quad [5]$$

ASCE (2014) and Hakhamaneshi et al. (2016) adopted the R_d concept and defined the performance level of structures based on R_d.

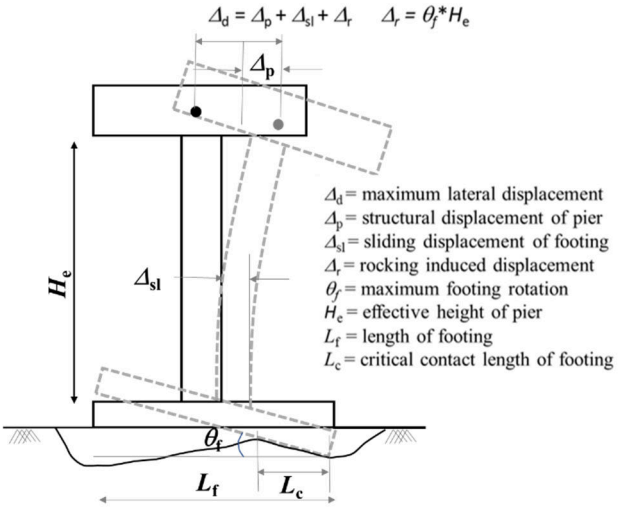

Figure 3. An SDOF structure showing three components of lateral displacements: Δ_p, Δ_{sl}, and Δ_r.

3.2 Rocking-induced Residual Settlement

The rocking-induced residual settlement (w_{res}), a major concern when the rocking mode is enabled, is one of the critical performance indicators in the present PBSD. Deng et al. (2014) suggested an empirical equation for w_{res}:

$$w_{res} = C_{sett} L_f \theta_{cum} \quad [6]$$

where C_{sett} and θ_{cum} is the settlement coefficient and cumulative footing rotation. The value of C_{sett} is empirically obtained from field tests in cohesive soil (Sharma and Deng 2020), while values in cohesionless soil are also available in the literature.

Values of w_{res} from Equation 6 are an envelope that encloses most of the settlement data obtained from cyclic and snap-back tests in cohesive soil in the field. It is difficult to estimate θ_{cum} owing to the variability of ground motions.

Except in long-duration large earthquakes, it might be reasonable to consider that a bridge or building experiences two full cycles of rotations equal to the design footing rotation θ_f (Deng et al. 2014). Then, Equation 7 may be adopted:

$$w_{res} = 4C_{sett}L_f\theta_f \quad [7]$$

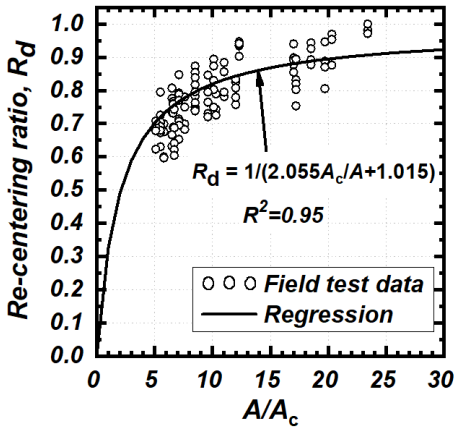

Figure 4. Empirical correlation between R_d and A/A_c

4 PBSD PROCEDURE

The PBSD procedure is described int this section. This method is applicable to standard ordinary bridges with seat type abutment having some conditions explained in Sharma (2019). The pier is assumed to be fixed to the bent cap beam for a single column pier bridge. The piers may be hinged at the top to the bent cap beam in case of multiple-columns piers supporting at the mid-span bridge. The transverse resistance of shear keys is neglected. The pier is considered elastic. Figure 5 presents a flowchart of the PBSD procedure.

5 DESIGN EXAMPLES

Sanguinetti Bridge (37°58'27.0"N 120°21'36.3"W) located in Sonora County, CA, is redrawn in Figure 6 (State of California 1973). A site classification C is assumed based on available soil information (Caltrans 2020). The footing was designed as a conventional fixed base with a footing size 6.7 m × 6.7 m which is much larger than would be required for the ultimate states of the underlying soil.

This research assumes that the bridge is located at a cohesive soil site with their bottoms resting on silt (MH) with a shear strength of 80 kPa and unit weight of 18.5 kN/m^3, since this MH soil site was adopted in the preceding field tests. The embedded depth of footing is 2.0 m as in original design. The foundation is assumed to be rocking along the transverse axis; the foundation length in the rocking direction will be redesigned following the proposed PBSD framework.

The dimension and properties of the as-built superstructure are reused in this example. The step-by-step procedure produces the following results.

1. The yield moment capacity of the as-built pier is M_{c_p} = 16.5 MN-m. Each pier assumed 95.8 kN axial load, half of the total weight of the superstructure.

2. The bridge is assumed to be located in a stiff clay site in Vancouver, BC, Canada. The medium to stiff clay is defined as Soil Profile Type III in CSA (2019). The spectral acceleration is selected according to CSA (2019) which corresponds to 2% probability of exceedance in 50 years with a return period of 2,475 years (Figure 7a). The displacement response spectra were calculated from acceleration response spectra (Figure 7b) Assume that the bridge is located far from any major faults, and therefore α of 0.5 is used.

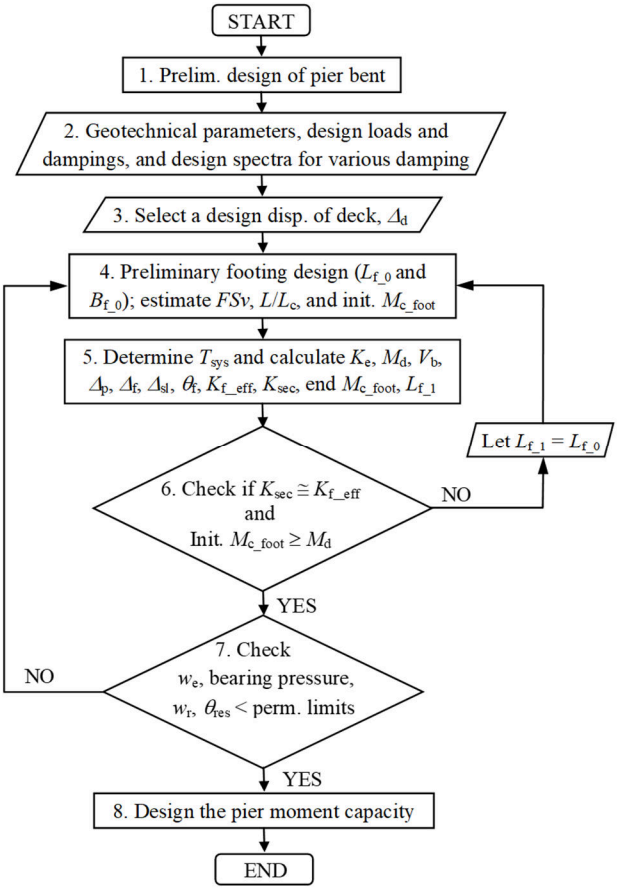

Figure 5. Flow chart of the PBSD procedure for rocking shallow foundation

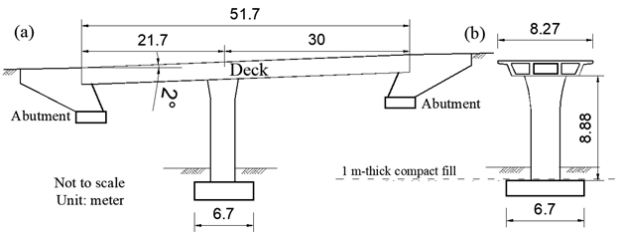

Figure 6. (a) Longitudinal; (b) transverse profiles of as-built Sanguinetti Bridge.

3. The design Δ_d is taken as 0.20 m (γ_m =2.25%), which is less than the allowable drift recommendation CSA (2019). This is also less than $0.2M_{c\_p}$ / (m·g) and the minimum seating width i.e., 0.3 m (CSA 2019).

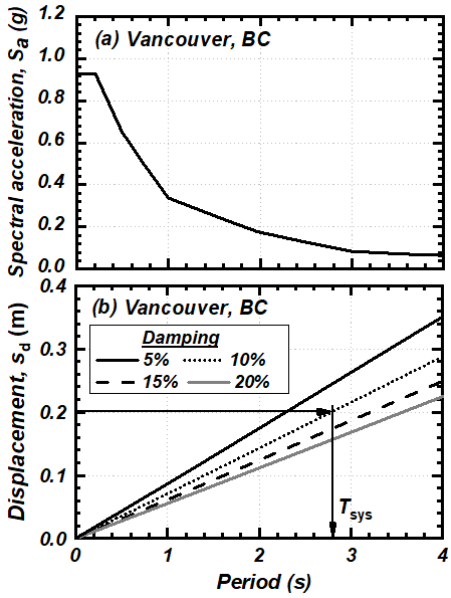

Figure 7. (a) 5% damped acceleration response spectra and (b) design displacement spectra in Vancouver site

4. Initially, a trial L_f = 4.0 m and L_f/B_f = 1.3 are assumed, where L_f is the length in the transverse direction. The trial values are based on the minimum FS_v required for bearing capacity of the footing. The design is intended to maintain the critical contact area ratio, A/A_c of about 8 to 10 to have the improved performance in R_d and w_{res} (Deng et al. 2014). The initial M_{c_foot} is 4.50 MN-m.

5. Assume ξ_p = 5% and ξ_f = 10%. The value of ξ_f is taken as ξ_{hys} for this design displacement.

a. The design period of the system (T_{sys}) read from displacement response spectra (Figure 7) is 2.8 s given Δ_d and ξ_{hys}.

b. K_e = 200 MN-m.

c. M_d = 4.52 MN-m and V_b = 509 kN. The lateral stiffness of the pier is K_p = 83.2 MN/m. Then the structural deformation of pier: Δ_p = 6.14 mm. The lateral deflection of the pier is only $0.03\Delta_d$. Then, the lateral displacement caused by footing:

$$\Delta_f = \Delta_d - \Delta_p = 193.9 \text{ mm}$$

d. Check ξ_{sys} using Equation 1: ξ_{sys} =9.85 %, which is close to the initial ξ_{sys} of 10%.

e. Horizontal stiffness of footing is K_{fh} = 107 MN/m (Gazetas 1991). The sliding displacement is Δ_{sl} = 4.77 mm. The small Δ_{sl} confirms that the system displacement is rocking dominated.

f. Calculate Δ_r = 189.1 mm. Then calculate the footing rotation: θ_f = 0.021 rad.

g. K_{f_eff} = 212 MN-m, where M_d = 4.52 MN-m.

h. The secant stiffness of the foundation given L_f, m, and θ_f (=θ_{max}) is calculated from Equations 2 and 3: K_{sec} = 165 MN-m.

i. The final moment capacity of the footing: M_{c_foot} = 4.52 MN-m. The length of the footing is back-calculated: L_f = 4.05 m.

6. The value of K_{sec} (in Step 5h) differs from K_{f_eff} (in Step 5g), and therefore iteration should be performed to satisfy the following condition: a. $K_{sec} \cong K_{f\_eff}$, b. Initial $M_{c\_foot} > M_d$, in order to have adequate stiffness and rocking capacity respectively, and (c) L_f in Step 4 $\cong$ L_f in Step 5i. All three conditions are satisfied after 7 iterations. The dimensions of the footing after iterations are as follows: L_f = 4.15 m, B_f = 5.40 m.

7. The elastic settlement based on the formulas in AASHTO (2011) is w_e = 2.4 cm. The allowable settlement recommended by AASHTO (2011) is 0.04×Deck length of bridge/2 = 10.3 cm. In addition, the average bearing pressure on the footing is 115 kPa (= mg/ ($2B_fL_f$)), unlikely to cause significant consolidation settlement that exceeds the serviceability limit.

a. The factored vertical load is calculated considering a dead load factor = 1.5 and a live load factor = 1.5 to account for the uncertainties in loads. The resistance factor for the ultimate bearing capacity is taken as 0.45 for uncertainties in soil properties. The ratio of the factored bearing capacity to the factored vertical load is 2.0, greater than the minimum threshold value (i.e. 1.0).

b. The settlement coefficient for the given A/A_c = 8.6 is C_{sett} = 0.032. The rocking-induced residual settlement from Equation 6 is w_{res} = 1.14 cm. This w_{res} is much less than w_e. In addition, the normalized settlement (i.e. $2w_{res}/L_f$) is 0.55%. The normalized w_{res} meets the settlement criterion.

c. As the moment-to-shear ratio (H_e/L_f) of 2.14 is greater than 1.0, the system will be rocking dominated. This indicates that sliding will be minimal. The sliding calculated in Step 5e normalized by L_f is only 0.12%.

d. The re-centering ratio for the given A/A_c = 8.6 is R_d = 0.8. According to Hakhamaneshi et al. (2016), R_d = 0.8 for rectangular footing can satisfy the immediate occupancy (IO) performance level. The residual rotation is θ_{res} = 0.005 rad. The residual drift ratio is 0.5%, less than allowable γ_{res} 0.6% for lifespan bridge (CSA 2019).

In summary, after seven iterations, the foundation design (i.e. L_f = 4.15 m, B_f = 5.40 m) meets all the performance levels and criteria for elastic settlement and bearing capacity at the normal operation condition.

6 PERFORMANCE FROM NONLINEAR TIME HISTORY ANALYSES

The performance of foundations designed by PBSD was verified by nonlinear time history analyses using a suite of earthquake motions. A two-dimensional single-column bridge model was developed in the OpenSees platform. The soil-footing interaction was modeled with the beam-on-nonlinear-Winkler-foundation (BNWF) method as shown in Figure 8. As shown in Figure, the q-z elements were used to simulate the rocking behaviour, while the p-y and t-z elements were to capture the passive resistance due to embedment and sliding frictional resistance, respectively. Input parameters for q-z, p-y, and t-z elements were obtained from the ultimate capacities (Qult, Pult, and Tult = ultimate bearing capacity, horizontal passive resistance, and horizontal sliding resistance, respectively) and the displacement at a half of the ultimate capacities (i.e. z50q, z50p, z50t). More details are presented in Sharma et al. (2022).

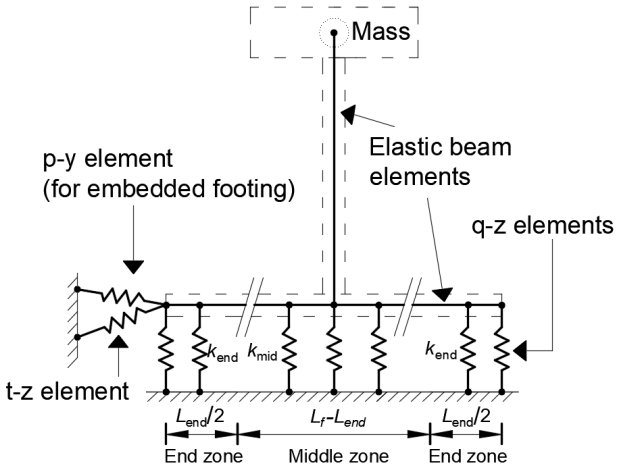

Figure 8. Beam-on-nonlinear-Winkler-foundation model for nonlinear time history analyses.

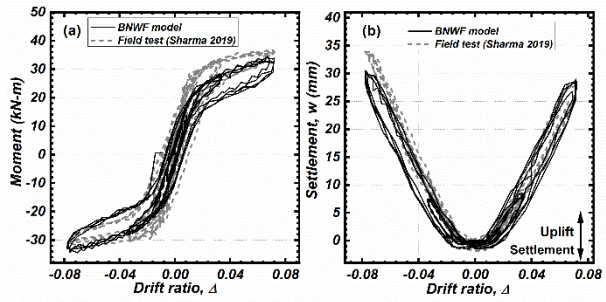

Figure 9. Comparison between BNWF model and field test results for slow lateral cyclic loading at a cohesive soil site: (a) rocking moment vs. footing rotation curves, and (b) settlement vs. footing rotation curves.

The BNWF model was validated against field cyclic tests. As shown in Figure 9, the numerical model slightly underpredicted the maximum moment during loading (positive moment), whereas the discrepancy became negligible in the opposite direction. Figure 9 suggests that the numerical model not only simulated the maximum moment of the system but also reasonably predicted the energy dissipation. The numerical model reproduced the settlement vs. rotation curve from the field test both in terms of settlement (or uplift) per cycle and total settlement.

6.1 Performance Evaluation

Performance of the designed foundation in cohesive soil was evaluated using nonlinear time history analyses with 15 ground motions (Figure 10), which were retrieved from the online database (PEER 2020). The selected motions were modified by SeismoSoft (2020) to match the displacement spectra at 10% damping (Figure 11). The numerical model developed against cyclic load tests was modified according to the dimensions of the redesigned footing. The value of G and k_{end}/k_{mid} adopted as 5.3 MPa and 4.0, respectively to make the rocking period of the model similar to the design period considered. The size of footing ($L_f \times B_f$) is 4.15 m × 5.40 m. The column height (H_c) is 6.77 m and the bridge deck weighs 95.8 kN.

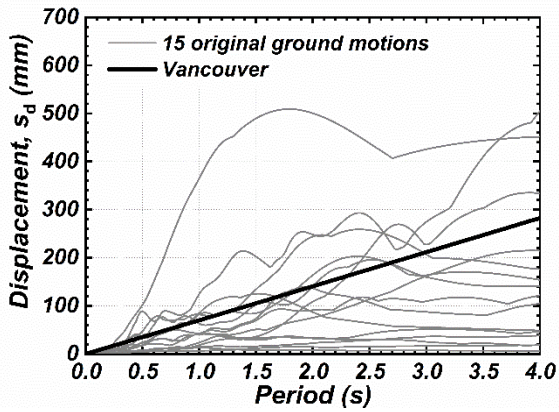

Figure 10. Design displacement response spectra and displacement response spectra of 15 original ground motions.

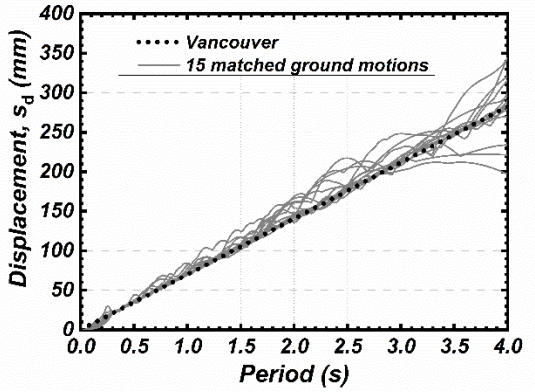

Figure 11. Displacement response spectra corresponding to 10% damping ratio and the spectra of 15 matched ground motions.

Figure 12 summarizes the results of γ_m, γ_{res} and w_{res} obtained from numerical modeling, along with values considered in the PBSD. Figures 12a shows that the difference between computed γ_m and PBSD-target γ_m ranged from 20% and 30%, which is deemed acceptable. Figures 12b shows that computed γ_{res} is less than values from the PBSD. The value of θ_{res} in PBSD was calculated which is empirically developed from field cyclic loading. Cyclic loading tended to result in large θ_{res}. In the time history analysis, the seismic load attenuates significantly after reaching the peak value and usually helps re-center the footing. As seen in Figure 12c, computed w_{res} are less than the values from PBSD.

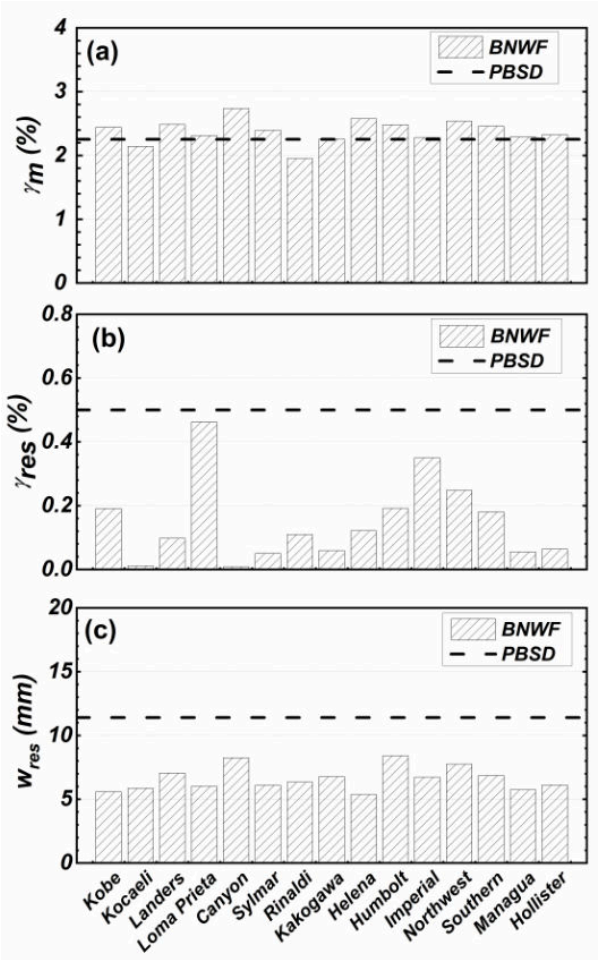

Figure 12. Performance indicators obtained from BNWF model and the PBSD method: (a) γ_m, (b) γ_{res}, and (c) w_{res}

7 CONCLUSIONS

This study presents a PBSD framework for rocking shallow foundations of ordinary bridges built in cohesive soils. Following conclusions may be drawn.

1. This study adopted empirical equations of secant stiffness and hysteresis damping ratios of rocking foundations. These correlations are crucial input to the PBSD framework. The empirical relationships of re-centering ratio vs. footing rotation and dynamic settlement coefficient vs. A/Ac were adopted to check the performance in terms of residual drift ratio and residual settlement.

2. The PBSD method was illustrated with two examples. A highway overpass bridge was re-designed with shallow foundations as if the foundations were located in a stiff clay. The maximum lateral displacement of the examples was set as 0.2 m and the as-built bridge deck and pier properties were used as the input. The redesign resulted in a footing dimension 4.15 m $\times$ 5.40 m, which was less than the as-built dimension and still satisfied the performance criteria set in this study.

3. The performance of the bridge pier was validated using nonlinear time history analyses of a SDOF soil-foundation-structure model. A numerical model was developed and calibrated against field test results. Numerical results suggest that the PBSD method is able to achieve the intended performance level for the rocking foundation embedded in the cohesive soil.

8 ACKNOWLEDGEMENTS

The research is funded by Natural Sciences & Engineering Research Council of Canada under the Discovery Grants program (RGPIN-2014-04707). The second author is grateful to the China Scholarship Council (201908430042) for funding the visit to the University of Alberta.

9 REFERENCES

AASHTO. 2011. Guide Specifications for LRFD Seismic Bridge Design (2nd edn). American Association of State Highway and Transportation Officials: Washington, DC.

Adamidis, O., Gazetas, G., Anastasopoulos, I., and Argyrou, C. 2014. Equivalent-linear stiffness and damping in rocking of circular and strip foundations. *Bulletin of Earthquake Engineering*, 12(3): 1177–1200.

Algie, T.B. 2011. Nonlinear rotational behavior of shallow foundations on cohesive soil. PhD thesis, University of Auckland, New Zealand.

Ambrosini, R.D. 2006. Material damping vs. radiation damping in soil–structure interaction analysis. Computers and Geotechnics, 33(2): 86–92.

American Society of Civil Engineers (ASCE). 2014. Seismic Evaluation and Retrofit of Existing Buildings (ASCE/SEI 41-13). Reston, VA.

Billah, A., and Alam, M.S. 2016. Performance-based seismic design of shape memory alloy–reinforced concrete bridge piers. II: methodology and design example. Journal of Structural Engineering, ASCE, 142(12): 04016141.

Caltrans. 2019. Seismic Design Criteria, version 2.0. California Department of Transportation, Sacramento, CA.

Caltrans. 2020. Caltrans ARS Online (v3.0.2). (https://arsonline.dot.ca.gov/index.php?).

Canadian Standards Association (CSA). 2019. Canadian Highway Bridge Design Code, CAN/CSA-S6-14, Mississauga, ON.

Chatzigogos, T.C., Pecker, A., Yilmaz, T.M., and Dietz, M. 2011. Seismic Engineering Research Infrastructures for European Synergies: Report on Pseudo-dynamic test techniques with SSI, WP14-JRA3.

Deng, L., Kutter, B.L., and Kunnath, S.K. 2014. Seismic design of rocking shallow foundations: a displacement-based methodology. Journal of Bridge Engineering, ASCE, 19(11): 04014043-1.

EGBC. 2018. Performance based seismic design of bridge in BC, Engineers and Geoscientist British Columbia, Canada.

FEMA. 2005. Improvement of nonlinear static seismic analysis procedures. FEMA 440, Washington, DC.

Finn, W.D.L. 2018. Performance based design in geotechnical earthquake engineering, Soil Dyn. Earthq. Eng., 114: 326-332.

Gazetas, G. 1991. Foundation Vibrations. Foundation Engineering Handbook, Chapter 15 (2nd edn), Fang, H-Y (ed.). V. N. Reinhold, New York, pp. 553-593.

Gazetas, G. 2019. Benefits of unconventional seismic foundation design. BGS 59th Rankine Lecture, https://www.youtube.com/watch?reload=9&v=pOXzqjTo34o&feature=youtu.be.

Hakhamaneshi, M., Kutter, B.L., Moore, M., and Champion, C. 2016. Validation of ASCE 41-13 modeling parameters and acceptance criteria for rocking shallow foundations. Earthquake Spectra, 32(2): 1121-1140.

NBCC. 2010. National Building Code of Canada, 13th Ed., National Research Council of Canada, Ottawa, ON.

NCHRP. 2010. LRFD design and construction of shallow foundations for highway bridge structures, Report 651, Transportation Research Board, NRC, Washington, DC.

NZS. 2004. Structural Design Actions, Part 5: Earthquake actions New Zealand. NZS 1170.5, Standards New Zealand, Wellington, N.Z.

Pacific Earthquake Engineering Research Center (PEER). 2020. NGA West 2, https://ngawest2.berkeley.edu/.

Sadan, O.B., Petrini, L., and Calvi, G.M. 2013. Direct displacement-based seismic assessment procedure for multi-span reinforced concrete bridges with single-column piers. Earthquake Engineering and Structural Dynamics, 42(7): 1031-1051.

Seismosoft, 2020. Seismomatch, https://seismosoft.com/products/seismomatch/.

Sharma, k. 2019. Field investigation and performance-based seismic design of rocking shallow foundations in cohesive soil, PhD Thesis, Department of Civil and Environmental Engineering, University of Alberta, AB, Canada

Sharma, K. and Deng, L. (2021) Effects of loading obliquity on field performance of rocking shallow foundations in cohesive soil, Géotechnique 71 (4): 320-333.

Sharma, K. and Deng, L. 2019. Characterization of rocking shallow foundations on cohesive soil using field snap-back tests, J. Geotech. Geoenviron., ASCE, 145(9): 04019058.

Sharma, K. and Deng, L. 2020. Field cyclic testing of rocking foundations in cohesive soils: foundation performance and footing mechanical response. Can. Geotech. J., 57(6): 828-39.

Sharma, K., Bin, J. and Deng, L. 2022. Performance-based seismic design of rocking shallow foundations in cohesive soil: Methodology and numerical validation. Soil Dynamics and Earthquake Engineering, 159, 107244.

Siddiquee, K. and Alam, M.S. 2017. Highway Bridge Infrastructure in the Province of BC, Canada. Infrastructures, 2(2): 7.

State of California. 1973. As built plans: U.C.D. cyclic overcrossing. Department of Transportation, Sacramento, CA.